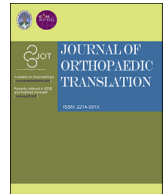


Contents lists available at ScienceDirect

## Journal of Orthopaedic Translation

journal homepage: [www.journals.elsevier.com/journal-of-orthopaedic-translation](http://www.journals.elsevier.com/journal-of-orthopaedic-translation)

# Complex joint-preserving bone tumor resection and reconstruction using computer navigation and 3D-printed patient-specific guides: A technical note of three cases

Kwok Chuen Wong<sup>\*</sup>, Louis Kwan Yik Sze, Shekhar Madhukar Kumta

Orthopaedic Oncology, Department of Orthopaedics and Traumatology, Prince of Wales Hospital, The Chinese University of Hong Kong, Hong Kong SAR, China

## ARTICLE INFO

## Keywords:

Joint-preserving tumor surgery  
Computer navigation  
Patient-specific guide  
Patient-specific implants  
Surgical accuracy  
Osseointegration

## ABSTRACT

In selected extremity bone sarcomas, joint-preserving surgery retains the natural joints and nearby ligaments with a better function than in traditional joint-sacrificing surgery. Geometric multiplanar osteotomies around bone sarcomas were reported with the advantage of preserving more host bone. However, the complex surgical planning translation to the operating room is challenging.

Using both Computer Navigation and Patient-Specific Guide may combine each technique's key advantage in assisting complex bone tumor resections. Computer Navigation provides the visual image feedback of the pathological information and validates the correct placement of Patient-Specific Guide that enables accurate, guided bone resections. We first described the digital workflow and the use of both computer navigation and patient-specific guides (NAVIG) to assist the multiplanar osteotomies in three extremity bone sarcoma patients who underwent joint-preserving bone tumor resections and reconstruction with patient-specific implants. The NAVIG technique verified the correct placement of patient-specific guides that enabled precise osteotomies and well-fitted patient-specific implants. The mean maximum deviation errors of the nine achieved bone resections were  $1.64 \pm 0.35$  mm (95% CI 1.29 to 1.99). The histological examination of the tumor specimens showed negative resection margin. At the mean follow-up of 55 months (40–67), no local recurrence was noted. There was no implant loosening that needed revision. The mean MSTs score was 29 (28–30) out of 30 with the mean knee flexion of  $140^\circ$  ( $130^\circ$ – $150^\circ$ ).

The excellent surgical accuracy and limb function suggested that the NAVIG technique might replicate the surgical planning of complex bone sarcoma resections by combining the strength of both Computer Navigation and Patient-Specific Guide. The patient-specific approach may translate into clinical benefits. The translational potential of this article:

The newly described technique enhances surgeons' capability in performing complex joint-preserving surgery in bone sarcoma that is difficult to be achieved by the traditional method. The high precision and accuracy may translate into superior clinical outcomes.

## 1. Introduction

In primary bone sarcomas surgery, surgeons perform resections with a tumor-free margin. Inaccurate resections with positive surgical margins resulted in local tumor recurrence and decreased patients' survival [1–3]. The bone defects following the resections have to be reconstructed to restore limb function. Bone resections with incorrect cutting planes may compromise the fitting of prostheses or allografts to the resection defects, leading to inferior limb function.

In selected extremity bone sarcomas, tumor resections may preserve

the articular end of the affected bones. The retained natural joints and ligaments enable a more normal joint function with better proprioception than patients with traditional joint-sacrificing tumor resections. Geometric resections using multiplanar osteotomies around bone tumors have been reported with the advantage of preserving more host bones for reconstruction and a better limb function [4–6].

However, it is difficult to correlate the tumor margins on preoperative CT and MR images to the actual tumor extent inside the bone in the operating room. The geometric bone resection is even more challenging if a custom tumor prosthesis reconstructs the bone defect. The intended

<sup>\*</sup> Corresponding author.

E-mail addresses: [skcwong@cuhk.edu.hk](mailto:skcwong@cuhk.edu.hk) (K.C. Wong), [louiskysze@gmail.com](mailto:louiskysze@gmail.com) (L.K.Y. Sze), [kumta@cuhk.edu.hk](mailto:kumta@cuhk.edu.hk) (S.M. Kumta).

<https://doi.org/10.1016/j.jot.2021.05.009>

Received 19 January 2021; Received in revised form 30 May 2021; Accepted 31 May 2021

bone resections require a high level of precision to accommodate the custom prosthesis as the error in bone resection magnifies with an increased number of resection planes around the tumor.

Computer navigation (CN) has been reported in assisting joint-preserving [7–10] and even geometric bone tumor resections [11–13]. Under real-time instant visual feedback related to the preoperative images, intraoperative navigation allows surgeons to identify the pathological structures and replicate the surgical plans accurately. However, currently available navigation systems do not support a navigated saw for the bone resections. Surgeons have to manually control the saw blade for the bone resection in an orientation guided under the navigation display's visual guidance. Operational errors may arise.

3D printed patient-specific guides (PSG) have recently been described as an alternative in replicating surgical plans in bone tumor surgery [14–18]. In contrast to CN, PSG has the advantage of providing a cutting platform that confines the sawblade to follow a pre-determined path. Therefore, the current PSG technique may be superior to the CN technique in bone tumor resections, particularly when the resection is geometric with multiple osteotomy planes [19]. Besides lacking real-time instant visual image feedback, the technique has a potential error in placing PSG on the pre-determined bone surface as there is currently no objective measurement in assessing the correct placement of PSG [14,19,20].

Using both CN and PSG may combine each technique's key advantage in assisting complex bone tumor resections. CN provides the visual image feedback of the pathological information and validates the correct placement of PSG. The PSG then enables accurate, guided bone resections. To our knowledge, this is the first study to describe the use and validation of the bone resection accuracy of the combined techniques (NAVIG) in three extremity bone sarcoma patients undergoing joint-preserving bone tumor resections and reconstruction with a patient-specific implant (PSI).

## 2. Methods

Between May 2015 and August 2017, three patients (average age: 13.7, 8–17) with primary bone sarcoma of lower extremities underwent chemotherapy and joint-preserving geometric guided resections and patient-specific prosthetic reconstructions (Table 1). The study was approved by the Clinical Research Ethics Committee of our hospital (Joint CUHK-NTEC: reference number: 2020.610).

Patients were included if they fulfilled the following criteria: (1) there was no evidence of tumor progression clinically or radiologically on MRI during preoperative chemotherapy; (2) at least 1 cm juxta-articular bone could be preserved after bone tumor resection to provide adequate bone for prosthetic fixation; (3) the main blood supply and nearby ligaments to the retained natural joints was not affected as shown on MRI; and (4) intraoperative guidance with both CN and PSG was thought to be necessary because of anticipated difficulties in achieving an accurate

geometric bone tumor resection and correct resection planes to accommodate a PSI.

### 2.1. Preoperative planning

The virtual surgical planning, the design, and manufacture of the custom prosthesis were performed while the patients continued preoperative chemotherapy. CT images (slices of 0.625 mm thickness) of the affected bone regions were acquired using a 16-detector scanner (LightSpeed, GE, Milwaukee, WI) at the same session of the CT-guided tissue biopsy during the initial diagnostic tumor workup. The CT images in DICOM (Digital Imaging and Communications in Medicine) format were imported into a medical image processing engineering software (Mimics 15.0, Materialise NV, Leuven, Belgium). The axial images were reformatted into coronal and sagittal views, and three-dimensional (3D) bone models were generated. The intraosseous tumor extent was mapped on CT images with supplementary information of MR images. The 3D bone tumor model was then generated for surgical simulation. By studying all the reformatted images and 3D models, surgeons defined bone resections planes with at least one cm tumor-free margin. The resection plan was a geometric, multiplanar (at least two planes) bone resection that preserved the natural knee/hip joints (Fig. 1A–F).

### 2.2. Patient-specific implants (PSI)

The MIMICS planning file was transferred to an implant engineer (Stryker Elstree, Stanmore Implants, UK) who then designed a PSI that matched precisely with the surgeon-defined bone resection planes and the bone defect's geometry (Fig. 2A–H). The design also considered the surgical approach and surrounding soft tissue to facilitate the placement of the PSI. Extracortical plates and screws were added to achieve the initial stable fixation to the residual juxta-articular bone. Hydroxyapatite was coated at the bone-implant junction to enhance the secondary osseointegration with host bone for implant longevity. Surgeons approved the PSI design before it was fabricated by the subtractive manufacturing method.

### 2.3. Patient-specific guides (PSG)

In MIMICS software, surgeons marked the bone surface footprints on the bone model that could be surgically exposed and near the planned bone resections (Fig. 3A). The engineer then transferred the bone model's CAD (Computer-Aided Design) files with footprints and the planned planes of bone resections to rapid prototyping (RP) engineering software (Magics RP, version 15.0, Materialise, Leuven, Belgium). The software allows editing and building CAD files to design a PSG that can be manufactured by 3D printing. The PSG design is composed of a few components (Fig. 3B and C): (1) a minimal of 15 mm width of cutting platforms

**Table 1**  
The demographics of the patients with the NAVIG-assisted geometric bone resection in long bone sarcoma.

Case	Diagnosis	Site	Number of osteotomies	Bone reconstruction	Navigation registration error (mm)	Operative time (minutes)	Mean maximum deviation errors	Follow-up periods (months)	Function (MSTS score)
1	High grade osteosarcoma	Right distal femur (lateral condyle)	3	PSI (Joint-preserving block)	0.4	235	1.6 mm (0.9–2.5 <sup>a</sup> )	66.8	29
2	Ewing sarcoma	Left proximal tibia (metaphysis)	3	PSI (Joint-preserving)	0.4	285	1.4 mm (1.2–1.7)	58.6	30
3	High grade osteosarcoma	Left femur shaft (extending to proximal and distal metaphyses)	3	PSI (double Joint-preserving and extendable)	0.8	309	1.6 mm (1.3–1.9)	40	28

NAVIG: Computer Navigation and patient-specific cutting Guide; PSI: Patient-Specific Implant; MSTS: Musculoskeletal Tumor Surgery with 30 as the highest score

<sup>a</sup> The maximum deviation error (2.5 mm) happened in the exit site of the most distal osteotomy at the posterior lateral femoral condyle. The cutting slit of the Patient-Specific guide could not control the tip of the oscillating saw in this osteotomy that had the longest bone cutting depth among the nine osteotomies in the study.

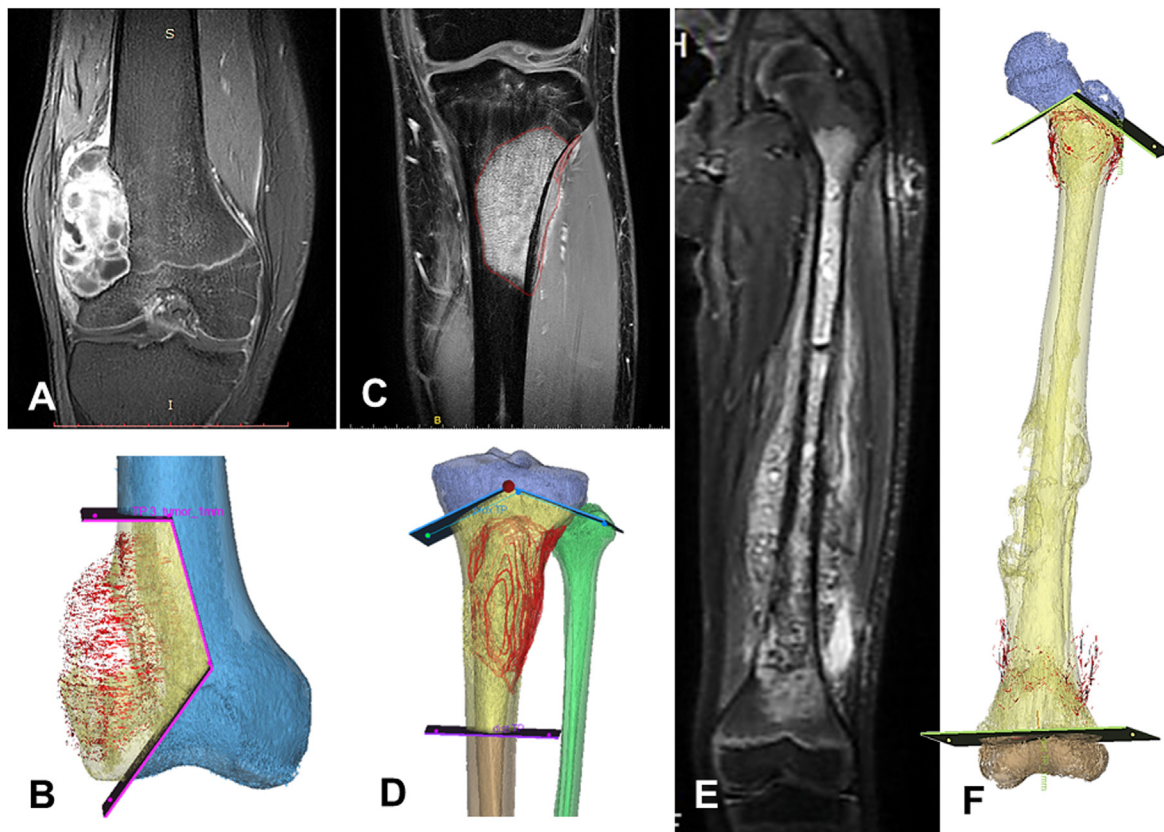


**Fig. 1.** A-F shows the coronal views of MR images and their respective three-dimensional (3D) bone-tumor models after image processing in Case 1 (A, B), Case 2 (C, D), and Case 3 (E, F). After analyzing all the image datasets and the 3D models, surgeons defined the geometric, multiplanar bone resections around the mapped tumor edge. The resection planes preserved the natural knee/hip joints while achieving at least one cm tumor-free margin.

or cutting slits that guided the oscillating saw along with the specific orientation of the intended resection. The slit was included if the surrounding soft tissue did not block its placement. It was 1.2 mm in width to accommodate an oscillating saw of 0.89 mm thickness for making an osteotomy; (2) contacting surfaces that conform to the bone surface footprints defined by the surgeons so that the PSG could consistently position on the bone surface; (3) 4 to 5 spherical holes of 1.8 mm diameter on the surface of the PSG that match with the tip of the navigation pointer. They were used as checkpoints to confirm the correct position of the PSG placement at the pre-determined bone surface footprints; (4) drill sleeves for placing Kirschner wires at the intersection between two osteotomy planes and secure the PSG to the bone after its correct placement was confirmed with navigation. The design also took into account the surgical approach or exposure, the nearby soft tissue at the defined position of PSI, and the direction of placing the PSI. Finally, the engineers combined different components of PSG in the RP software (Fig. 3D).

After the surgeons approved the final design, the PSGs and bone models were fabricated using the Fused Deposition Modeling (FDM) technique by a 3D printing machine (Fortus 400mc FDM system, Stratasys Inc., Eden Prairie, MN). A thermoplastic material, Acrylonitrile butadiene styrene (ABS), was used in the first two patients. The PSG and models made of ABS were sterilized at low temperatures using hydrogen peroxide. The third patient used another thermoplastic material, ULTEM™ resin that could be sterilized by high-temperature autoclaving. The surgeons practiced the placement of PSG on the bone models before the actual operation.

#### 2.4. Computer navigation (CN) planning

The engineering software allows advanced surgical planning like

bone resection simulation and patient-specific prosthesis and PSG design. However, the information could not be directly transferred to the navigation system for CN planning due to system incompatibility. The virtual surgical plan was integrated into the navigation system by using CAD to DICOM conversion as described previously [21]. In MIMICS software, the CAD models of the surgeon-defined resection planes, PSI and PSG were overlaid on the original CT images, which were exported as modified DICOM files. The original and modified DICOM files were then imported into a CT-based navigation system (Stryker Navigation System, OrthoMap 3D module, version 2.0, Stryker, Mahwah, NJ) for surgical planning. Automatic image fusion of the two datasets was performed. MR images were also fused with the CT images [22], and the tumor extent was outlined. The CAD models of the prosthesis and PSG were integrated according to their planned positions on CT images. This integration replicated and accurately defined the planned locations of the resection planes, implant, and PSG on the CT images in the navigation system (Fig. 4A–E).

#### 2.5. CN- and PSG-assisted bone tumor resection

Intraoperative techniques of computer navigation have been described [9,12,19]. The bone sarcoma was surgically exposed so that the tumor could be resected with cuffs of normal tissue as a tumor-free margin, and the locations of the planned osteotomies were clear of soft tissue for the placement of PSG. A patient tracker was attached to the bone in which the tumor was located. The navigation probe was calibrated to the navigation system. Image-to-patient registration was then performed using paired points and a surface matching algorithm to accurately match the operative anatomy and preoperative CT images. The registration allowed real-time tracking of the tip of the navigation probe's spatial location with the patients' anatomy on the virtual

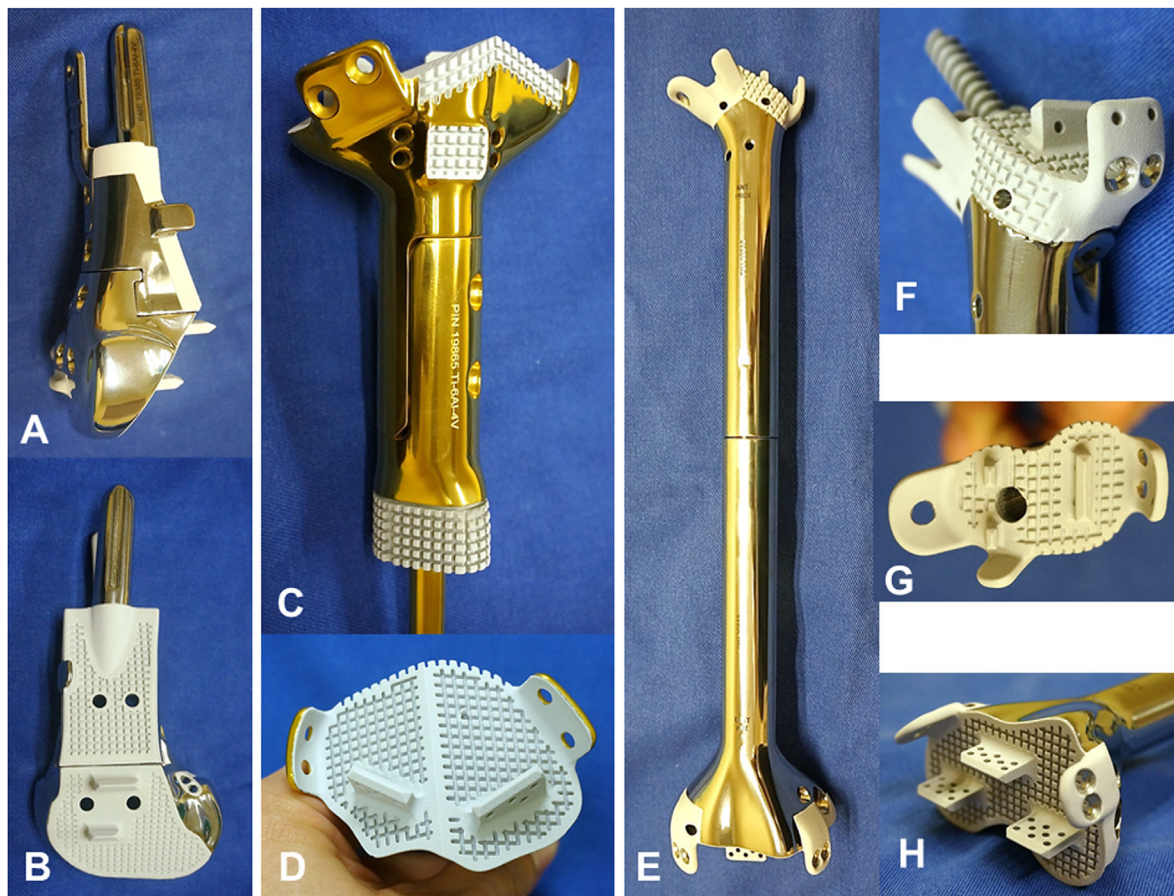


**Fig. 2.** A–H shows the custom Patient-Specific Implants (PSI) in Case 1 (A, B), Case 2 (C, D), and Case 3 (E–H). Engineers designed the PSI that matched precisely to the surgeons' defined resection planes in MIMICS software. The cemented intramedullary stems, extracortical plates, and cutting fins provided the primary implant fixation while the serrated, hydroxyapatite-coated surface of the implant junctions enhanced the implant osseointegration to the host bone. Suture holes could be included to reattach tendon/ligaments. The digital surgical planning workflow allowed on-demand implant design that enabled the primary stable implant fixation with secondary osseointegration at bone-implants for durable implant longevity.

preoperative CT/MR images. The registration accuracy was verified by tracing the exposed bone or cartilage surface with the navigation probe. The PSG was placed and moved on the planned bone surface footprints until its position was subjectively stable. CN was then used to check the correct placement of the PSG by placing the tip of the navigation probe at the checkpoints of PSG (Fig. 5A–D). The position of PSG was adjusted until the checkpoints matched their planned positions on the navigation display. Kirschner wires were inserted via the drill sleeves to fix the PSG to the bone. The planned osteotomies' sites and orientation were also confirmed with CN before the precise osteotomies were performed by an oscillating saw guided by the PSG. A complementary prosthesis template was placed at the bone defect to assess the initial PSI fitting and prepare the bone trough to accommodate cutting fins (Fig. 6A–F). The bone defect was then reconstructed with the PSI and stabilized with extracortical plates and screws. Therefore, the combination of CN and PSG techniques enabled the surgeon to replicate complex osteotomies exactly as the virtual surgical plan.

To assess the surgical accuracy of the NAVIG technique, (1) the fitting of the PSI to the remaining bone was recorded at the surgery; (2) CT scans were performed on the resected bone tumor specimens with the same protocol as the preoperative CT scans. The generated 3D bone models were co-registered to that of the MIMICS software's surgical planning to measure the achieved bone resections' maximum deviation errors.

Postoperatively, the patients had early physiotherapy with joint mobilization and protected weight-bearing walking. Chemotherapy was resumed two weeks after surgery when the wounds healed. All patients were followed regularly at one month, two months, every three months

for two years, every six months until five years. Clinical examination was performed to look for local tumor recurrence, and limb functions were recorded using MSTs scores [23]. Plain radiographs of the operated areas were taken at each follow-up to assess the healing at the bone–implant junction and the remaining juxta-articular bone viability. Intraoperative and postoperative complications were also recorded.

### 3. Results

All three cases could be performed under the NAVIG technique as planned. The mean operative time was 276 min (range: 235–309 min). The mean registration error for the navigation procedure was 0.5 mm (0.4–0.8). The correct placement of PSG could be verified with the PSG built-in checkpoints under the navigation feedback before implementing PSG-guided bone resections. All PSI matched well to the remaining bone at the bone–implant junctions. The mean maximum deviation errors of the nine achieved bone resections were  $1.64 \pm 0.35$  mm (95% CI 1.29 to 1.99) (Table 2). The histological examinations of the surgical margins in all resected tumors were negative. No wound complication or infection was noted. At the mean follow-up of 55 months (40–67), there were no local recurrence nor distant metastases. The plain radiographs showed all retained juxta-articular bones were viable without osteonecrosis, and the osseointegration was present at all bone–implant junctions except one at the greater trochanter in Patient 3. There was no implant loosening that needed revision. The mean MSTs score was 29 (28–30) out of 30. The mean knee flexion was  $140^\circ$  ( $130^\circ$ – $150^\circ$ ).

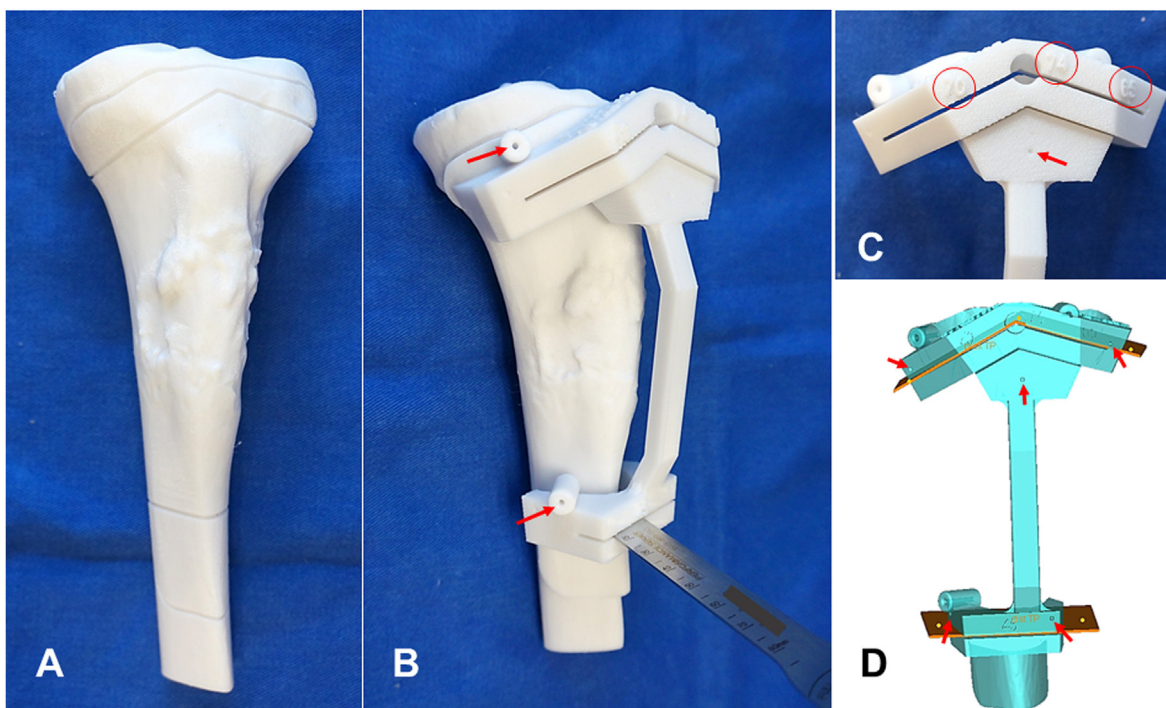


**Fig. 3.** A-D (A) The proximal tibia bone model of Case 2 had markings of the planned resection planes' sites and seating footprints of the Patient-Specific Guide (PSG) (B) The PSG had the cutting slits that confined the specific orientation of the oscillating saw for intended osteotomies. Also, it had drill sleeves (red arrows) for 1.6 mm Kirschner wires to stabilize the PSG to the bone after computer navigation confirmed the correct positioning of the PSG (C) The correct intraoperative positioning of the PSG was confirmed with the computer navigation by the tip of the navigation pointer touching at the checkpoints (red arrows) on the PSG. The depth of the osteotomies (red circles) was printed next to the cutting slits (D) The Computer-Aided Design (CAD) model of the PSG had the cutting slits matched to the planned osteotomies and the checkpoints (red arrows) for navigation confirmation of the correct PSG positioning. Surgeons approved the CAD model before the PSG was 3D-printed.

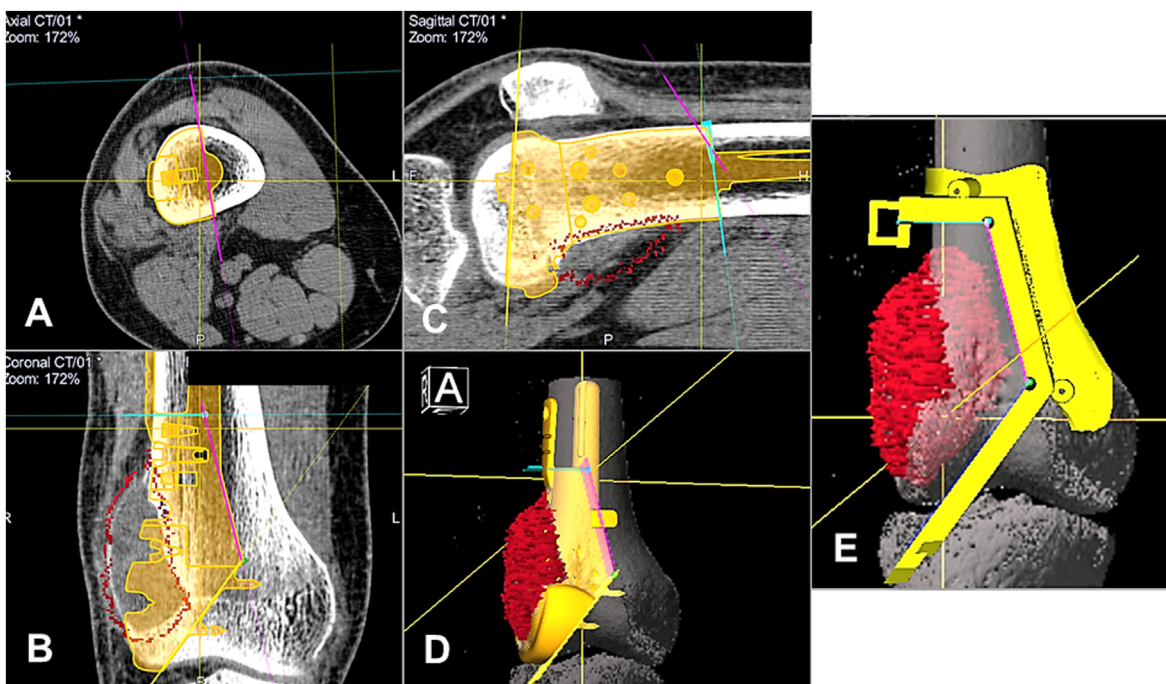


**Fig. 4.** A-E shows the preoperative navigation planning in Case 1 after the virtual tumor resection, Patient-Specific Implant (PSI), and Patient-Specific Guide (PSG) designs were indirectly integrated into the navigation system. The axial (A), reformatted coronal (B) and sagittal (C) views of CT images and the 3D bone model with PSI (D) defined the planned osteotomies that were marked by a “plane” in the system (E) The Computer-Aided Design model of the PSG was also integrated similarly into the 3D bone-tumor model.

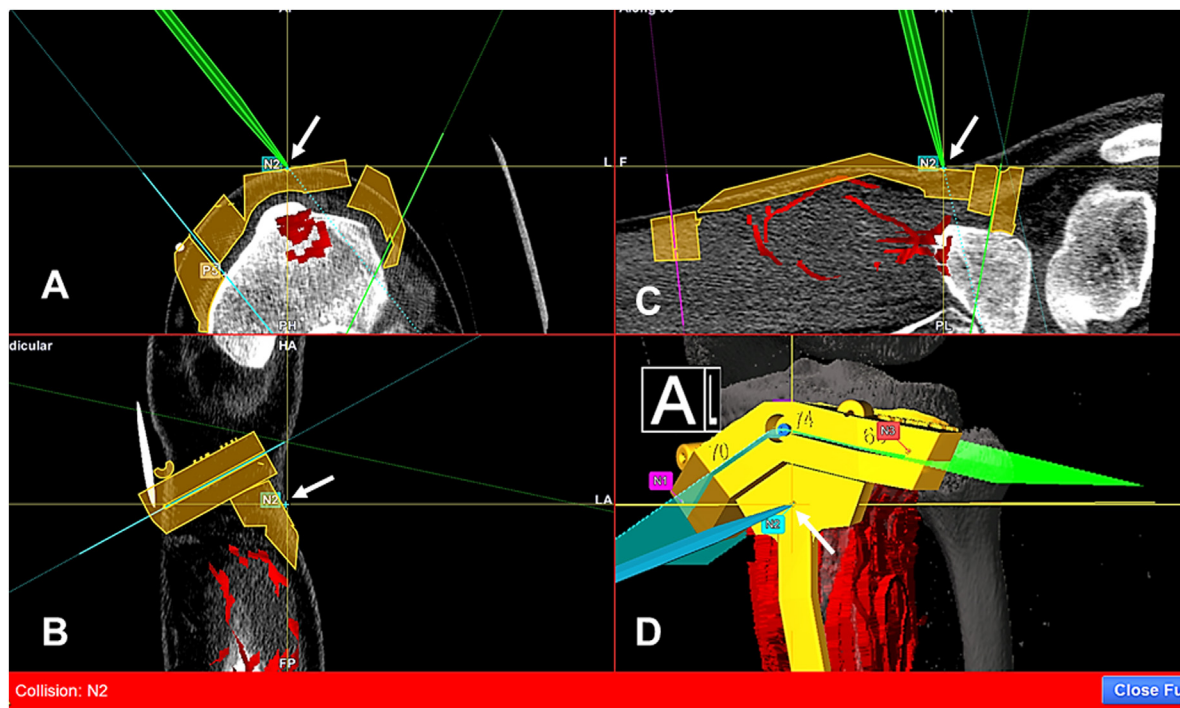


**Fig. 5.** A–D shows the intraoperative computer navigation guided positioning of the Patient-Specific Guide (PSG) in Case 2. The virtual tip of the navigation pointer (white arrows) coincided with the checkpoint “N2” on the PSG on the axial (A), coronal (B), and sagittal (C) views and the 3D model (D) on the navigation display. There was a continuous beep sound, and the bottom bar of the navigation display turned red when the tip of the navigation pointer touched the checkpoints. Other checkpoints were checked similarly on the PSG, thereby verified the correct PSG positioning.

### 3.1. Case 1

A 16-year-old boy had high-grade osteosarcoma involving the lateral condyle of the right distal femur. Joint-preserving tumor resection was planned to retain his knee joint instead of performing a conventional distal femur tumor resection that would sacrifice most of his normal distal femur, knee ligaments/meniscus, and the articular surface of the normal proximal tibia to restore knee articulation. Joint-preserving, geometric tumor resection with a surgical bone margin of at least 1 cm was virtually performed in MIMICS software (Fig. 1A). The bone defect's geometry and the PSI were re-created by overlaying the mirror image at the opposite normal femur. As the surgical approach was lateral, the PSI was designed to be two separable components that could be assembled intraoperatively to ease the implant placement (Fig. 2A and B). PSG was designed and 3D-printed to replicate the planned resection planes intraoperatively. The virtual surgical plan was transferred to the computer navigation system.

The right distal femur osteosarcoma was exposed laterally after the unaffected quadriceps muscle and the right knee's posterolateral ligament complex were free from the tumor. The bone surface near the planned resection sites was exposed with reference to the 3D-printed planning bone model. An image-to-patient registration was performed with a < 1 mm registration error after a patient tracker was attached to the femoral shaft. The correct placement of PSG was determined by the navigation probe's tip touching the PSG checkpoints that matched to their corresponding checkpoints on the navigation display. The PSG was then stabilized with 1.6 mm Kirschner wires. The PSG-guided resection planes were further confirmed under navigation guidance before the actual osteotomies (Fig. 7A and B). The remaining bone was viable with bleeding. A 3D-printed complementary template was placed at the resected surface to assess the PSI fitting and make the bone trough accommodate the cutting fins. The PSI fitted well to the achieved bone defect and was stabilized with screws and a cerclage wire (Fig. 7C). The posterolateral knee ligament complex and lateral head of gastrocnemius

muscle were reattached to the sutures holes on the PSI. He underwent physiotherapy with gradual knee mobilization and weight-bearing walking. He could flex his knee to 140° (Fig. 7D and E).

### 3.2. Case 2

A 17-year-old boy had an Ewing sarcoma involving the metaphysis of the left proximal tibia. Joint-preserving tumor resection with a biplanar osteotomy was virtually planned around the dome-shaped, intramedullary extent of the tumor at the proximal tibia (Fig. 1D). The remaining proximal tibia bone provided better rotational stability and more bone stock for the PSI's initial fixation with plates and screws (Fig. 2C and D). A PSG was designed and 3D-printed to replicate the planned osteotomies by considering the surgical approach and the surgeon-defined footprints (Fig. 3A and B).

With an anteromedial surgical approach, the Pes Anserinus and the patella tendon were released to expose the proximal tibia. The soft tissue at the planned PSG's footprint was elevated subperiosteally. An image-to-patient registration was performed and verified after a patient tracker was attached to the tibial shaft via a clamp. The PSG was correctly positioned after verified with the PSG's checkpoints under navigation guidance (Fig. 8A). The PSG was stabilized with 1.6 mm Kirschner wires. The osteotomies were performed via the cutting slits of the PSG (Fig. 8B). The 3D-printed prosthesis template confirmed the accurate osteotomies and the bone troughs to accommodate the cutting fins were prepared. The proximal component of the PSI was fixed to the remaining proximal tibia with screws and the cemented tibial stem of the distal component of the PSI was inserted in a usual fashion. The two components were assembled with bolt screws (Fig. 8C). The medial gastrocnemius muscle flap was elevated to cover the prosthesis's anterior aspect, where the extensor mechanism of the patellar tendon was also reconstructed. A partial-thickness skin graft was required to cover a part of the muscle flap. He was given postoperative radiotherapy despite a negative resection margin because of only 75% chemonecrosis on the resected

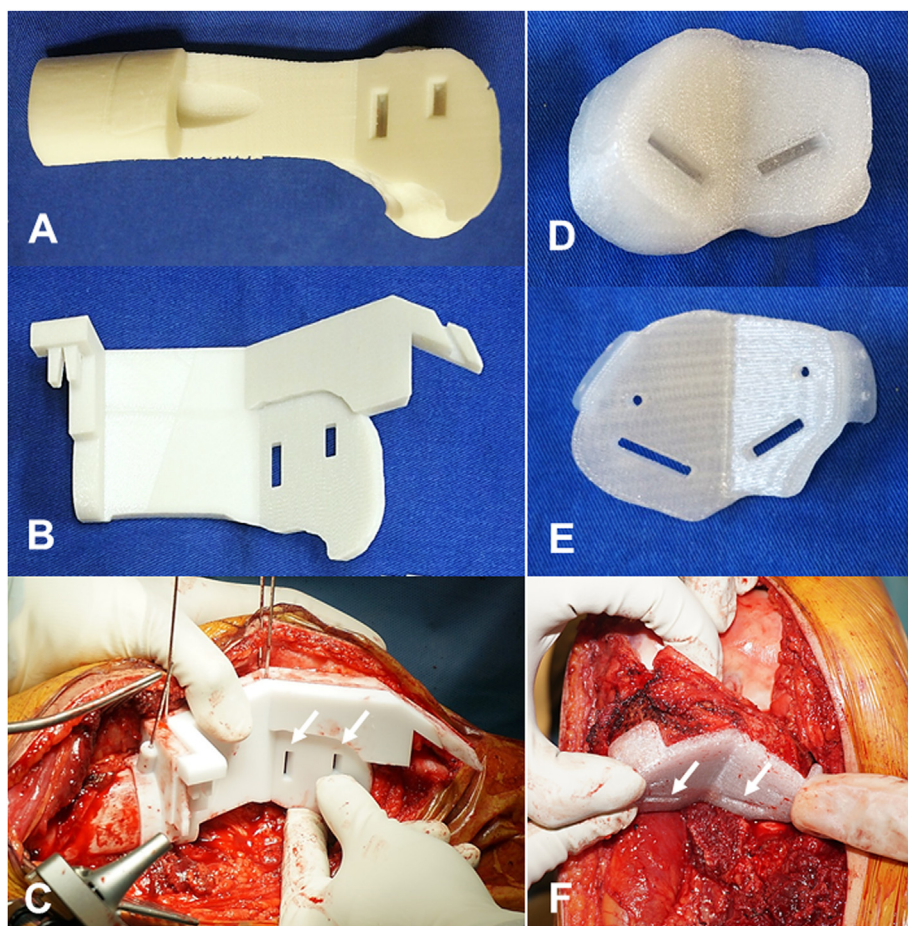


**Fig. 6.** A–F shows the 3D-printed model of the remaining distal femur (A) after bone tumor resection in Case 1, his complementary prosthesis template (B) had the same junctional geometry of the bone defect (C) During the surgery, the template was placed at the resected bone end to assess the resection accuracy and the Patient-Specific Implant (PSI) fitting. Bone troughs (white arrows) at the remaining bone were prepared via the template to accommodate PSI's cutting fins. In Case 2, the remaining proximal tibia (D) and the prosthesis template (E) were similarly 3D-printed (F) The template fitted well to the bone defect intraoperatively that verified the accurate bone resection and well-matched PSI. Bone troughs (white arrows) were also prepared via the template.

**Table 2**  
The deviation errors of computer navigation-assisted bone resection in long bone sarcoma.

Studies	Number of patients (osteotomies)	Mean age	Bone reconstruction	Mean maximum deviation errors
Aponte-Tinao et al. (2013) [11]	5 patients (18 CN)	56 (42–71)	Allograft	2.43 ± 1.8 mm
Bosma et al. (2018) [20]:	8 procedures (14 CN)	NA	NA	3.6 ± 2.1 mm
Cadaveric study	8 procedures (14 NAVIG)	NA	NA	2.0 ± 1.0 mm
Zhang et al. (2020) [26]	10 patients (16 CN)	26.6 (12–52)	Not mentioned	2.52 ± 1.38 mm
Current study	3 patients (9 NAVIG)	13.7 (8–17)	Custom Patient-specific implants	1.64 ± 0.35 mm

CN: computer navigation assistance; NAVIG: Computer Navigation and patient-specific cutting Guide; N/A: not applicable

specimen's histology. He could achieve full knee extension and flexion (Fig. 8D).

### 3.3. Case 3

An 8-year-old boy had high-grade osteosarcoma involving the left femoral shaft extending to proximal and distal femur metaphyses. Double joint-preserving surgery was planned to retain the knee and hip joints' growth for better leg function. The bone resection included a proximal

biplanar osteotomy at the trochanteric region and a distal intra-epiphyseal osteotomy (Fig. 1F). A minimally invasive extendable joint-preserving femur tumor prosthesis was designed (Fig. 2E–H). The NAVIG technique accurately replicated the surgical plan due to anticipated difficulty in the correct placement of PSG in the cylindrical femur bone. The CN could confirm the correct placement of PSG before implementing PSG-guided osteotomies.

A lateral surgical approach was used. The quadriceps muscle was elevated and reflected medially to expose the whole femur (Fig. 9A). The bone surface at the PSG's footprint was exposed subperiosteally while keeping the hip capsule and posterior knee capsule intact to avoid inadvertent injury to the blood supply to the femoral head and distal femoral epiphysis. An image-to-patient registration was performed and verified after a patient tracker was attached to the femur shaft. The PSG was correctly positioned after verified with the PSG's checkpoints under navigation guidance (Fig. 9B and C). After the PSG was stabilized with 1.6 mm Kirschner wires, the femur was osteotomized with an oscillating saw in an orientation guided by the PSG cutting platforms. Complementary prosthesis templates confirmed the PSI fitting and allowed the preparation of bone troughs at the remaining femur bone to accommodate the cutting fins. The PSI's proximal component was fixed to the femoral head by a 6.5 mm Hydroxyapatite (HA)-coated screw, and a 3.5 screw was added to fix the medial femoral neck (Fig. 9D). Iliopsoas and vastus lateralis insertion were also reattached to the suture holes of the PSI. The distal component of the PSI was then assembled to the proximal component. The remaining distal femur epiphysis was fixed to the distal component with screws.

The patient underwent one lengthening of 2 cm at 1.5 years after the surgery. At a follow-up of three years, he could achieve a full hip and knee range of motion. On the plain radiograph, the distal femur epiphysis

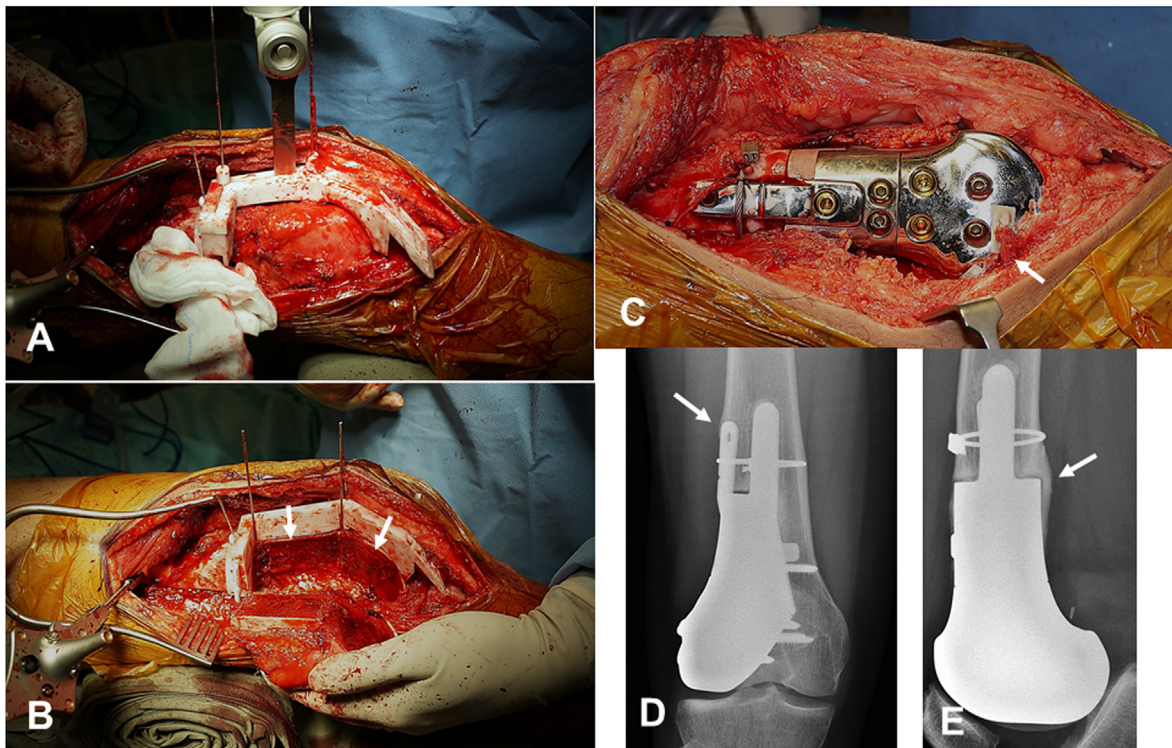


**Fig. 7.** A–E. In Case 1 (A) the right distal femur osteosarcoma was exposed via an anterolateral surgical approach. Computer navigation verified the correct placement of the Patient-Specific Guide that was then stabilized to the bone by Kirschner wires. The planned resection was performed by the oscillating saw via the cutting slits of the PSG (B) Precise geometric bone resection (white arrows) could be achieved (C) The Patient-Specific Implant (PSI) matched well to the bone defect. The PSI consisted of three components for ease of placement. The metaphyseal part, the proximal lateral extracortical plate, and the femoral condylar were connected with bolt screws. The PSI was stabilized by multiple screws, intramedullary cutting fins, and extracortical plates with cerclage wires. Suture holes were available at the PSI's lateral epicondyle for reattaching the knee joint's posterolateral ligament complex. Hydroxyapatite was coated at the bone–implant junctions for secondary osseointegration. The anteroposterior (D) and lateral (E) views of the plain radiograph of the knees showed good bone formation (white arrows) at the bone–implant junctions at three years after the surgery.

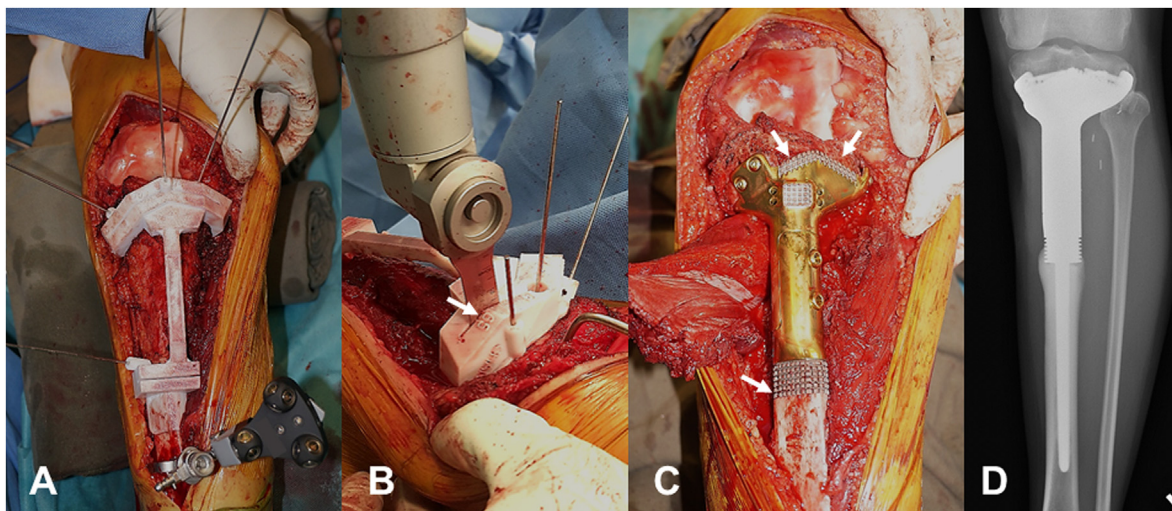


**Fig. 8.** A–D. In Case 2 (A) the left proximal tibia Ewing sarcoma was exposed via an anteromedial surgical approach. After the computer navigation verified the correct placement of the Patient-Specific Guide (PSG), the PSG was stabilized to the tibia bone by multiple Kirschner wires (B) The proximal tibia osteotomy was then performed by an oscillating saw via the cutting slits of PSG. The osteotomy depth was also 3D-printed next to the cutting slit for easy reference (white arrow) (C) The Patient-Specific Implant (PSI) fitted well at the bone–implant junction (white arrows). The medial gastrocnemius local flap was elevated to cover the PSI, and the extensor mechanism was reconstructed (D) The anteroposterior view of the tibia's plain radiograph showed good bone formation at the bone–implant junction without loosening at four years after the surgery.

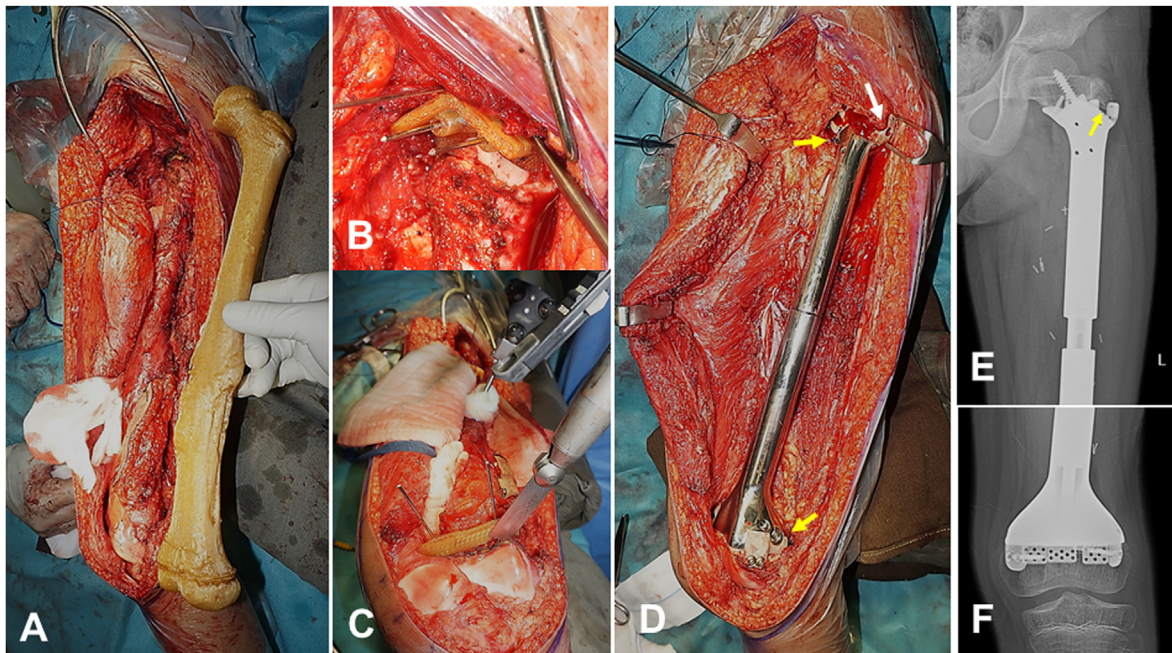


**Fig. 9.** A–F. In Case 3 (A) the left femur osteosarcoma was exposed via lateral approach and anterolateral approach at the femoral neck region. The exposure and the proximal resection preserved the vascular branches from medial and lateral circumflex vessels supplying the femoral head, while the distal resection preserved the middle geniculate vessels supplying the distal femur epiphysis. The femur bone replica was 3D-printed and sterilized for reference during surgical exposure. The Patient-Specific Guides were correctly placed and stabilized by Kirschner wires at the proximal osteotomy site (B), and the distal osteotomy site (C) after their positions were verified by computer navigation. (D) The Patient-Specific Implant (PSI) was fixed to the remaining femoral head and distal femoral epiphysis with extracortical plates and screws. As the small remaining greater trochanter could not accommodate screw fixation, the abductor insertion was sutured to the implant junction via the suture holes on the extracortical plates (white arrow). Iliopsoas tendon and gastrocnemius head tendons were reattached to the PSI suture holes (yellow arrows). Three years after the surgery, the anteroposterior view of the plain radiograph of the hip (E) showed viable and continuous growth of the femoral head. Some dysplastic growth was noted at the greater trochanter due to the tumor resection with its physis. The patient had no left hip pain with the non-progressive lucent line (yellow arrow). The anteroposterior view of the plain radiograph of the knee (F) showed continuous growth and expansion of the distal femoral epiphysis.

showed a continuous growth; the acetabular growth was retained as the femoral head grew, but there was evidence of dysplastic growth at the femoral neck after the resection of the physis at the greater trochanter (Fig. 9E and F).

#### 4. Discussion

A geometric resection using multiplanar osteotomies around a bone sarcoma may allow joint preservation while the remaining juxta-articular bone can be reconstructed with a better limb function [4–6]. However, the complex surgical planning translation is challenging when the bone resections have to achieve a negative margin and correct orientations if a prefabricated PSI is used for bone reconstruction [9]. To our knowledge, it was the first study to describe the digital workflow in surgical planning, PSI, and its PSG design in multiplanar joint-preserving surgery in paediatric and adolescent patients with bone sarcoma. The excellent surgical accuracy and limb function suggested that the NAVIG technique might replicate the surgical planning of complex bone sarcoma resections by combining each technique's strength. The patient-specific approach may translate into clinical benefits.

The current study has limitations. First, only a small case series without a control group and a definite conclusion cannot be drawn. However, the case series is the first clinical report about the use of both CN and PSG in assisting complex geometric resections in joint-preserving tumor surgery after good surgical accuracy was demonstrated in the cadaveric study using the same technique [20]. Our study served as a proof of concept and a technical note. Second, the excellent short-term limb function with PSI may deteriorate in time as aseptic loosening or mechanical failure were inevitable in tumor endoprostheses in the long run [24]. However, the joint-preserving PSI does not have articulating components like in traditional joint-sacrificing tumor endoprostheses.

We expect the limb function can be maintained if the solid osseointegration can be achieved at the bone–implant junctions. Third, the technique requires strict patient selection. The surgery may not be suitable for patients with bone sarcomas who are not good responders to neoadjuvant chemotherapy or have tumors involving the epiphysis. PSG may not be suitable in bone sarcomas with large extraosseous components that may hinder the PSG placement. Also, after the joint-preserving resections, the remaining juxta-articular bones have to be sufficient for stable implant fixation. Fourth, the high surgical accuracy level with the mean maximum deviation errors of less than 2 mm may not be clinically significant, especially when a usual 10 mm safe surgical bone margin is adopted for bone sarcoma resection. However, given that errors may magnify with increased osteotomy planes in geometric resections and bone reconstruction with a prefabricated PSI, the achieved surgical accuracy ensures the best fit without compromised local oncological control. Fifth, the technique requires the navigation facilities, surgeons' expertise in using both CN and PSG, and engineers' support in the design and manufacture of PSG and PSI. They are not readily available at most tumor centers and surgeons may not duplicate the NAVIG technique that requires meticulous seamless teamwork. With continued technology advancement, we expect a unified simplified workflow or even robotic assistance like joint arthroplasty [25] may be developed to reduce the learning curve and gain popularity of the technique.

The current study of using the NAVIG technique in joint-preserving tumor surgery showed that the nine achieved osteotomies' mean maximum deviation errors were  $1.64 \pm 0.35$  mm. The results were slightly better than the mean errors reported in previous studies using computer navigation alone (2.43–3.60 mm) [11,20,26] [Table 3]. The surgical accuracy of using the NAVIG technique was  $<2$  mm in the mean maximum deviation errors that were consistent with the only cadaveric study [20] [Table 3]. Given the potential errors in PSG placement on the

pre-determined bone surface [14,19,20], the CN procedure with sub-millimeter registration error might provide an objective assessment to confirm the correct placement of PSG, and therefore guided the correct orientation of the planned osteotomies. The complementary use of CN may help joint-preserving tumor surgery in long bones that are cylindrical shapes with insufficient bony landmarks or in geometric, multiplanar tumor osteotomies that require precision to accommodate a custom PSI. With the NAVIG technique in selected cases, more conservative bone resections that preserve native joints and ligaments may be achieved for reconstruction with a better limb function.

The rate of local recurrence (0%) was comparable to the rates (0%–9%) reported in other studies [9,27–30] in which patients with bone sarcoma underwent joint-preserving tumor surgery. It was also comparable with the rates (4%–9%) in other large cohort studies of surgically treated extremities bone sarcoma [31–35]. Our short-term results concluded that the joint-preserving tumor surgery was an oncologically safe and acceptable method of limb salvage surgery in selected patients with bone sarcoma. Recent case–control studies showed that CN facilitated negative resection margins and improved local control by reducing tumor recurrence in patients undergoing acetabular tumor resections [36,37]. The NAVIG technique may precisely replicate the surgical plan that ensures a negative resection margin and mitigates local recurrence even in complex geometric multiplanar sarcoma resections.

Implant fixation to the small juxta-articular bone is challenging in joint-preserving tumor surgery. No implant loosening was noted as the bone–implant junctions of all osteotomies except one achieved osseointegration. It was consistent with the other joint-preserving surgery studies with custom implants that no aseptic loosening developed in the residual epiphysis [9,38–40]. The good results were attributed to the patient-specific implant design conforming to the anatomy and cutting fins and extracortical plates with screws for primary implant fixation. The PSI matched well to the achieved osteotomies under the NAVIG technique. Stable primary implant fixation then allowed secondary osseointegration at the HA-coated bone–implant junctions. The subsequent leg shortening could also be corrected by minimally invasive lengthening in the custom extendable PSI. The preserved natural joint with nearby ligaments and leg length discrepancy correction supported the excellent limb function with the mean MSTS score of 29 and the mean knee flexion of 140°.

As the NAVIG technique enhances surgeons' ability to perform complex geometric resections, PSIs with improved design can be implanted. The 3D-printed PSIs have recently been applied for bone reconstruction with early promising results in bone tumor surgery [41–45], revision acetabular surgery [46,47], and craniomaxillofacial surgery [48]. 3D printing has the distinct advantages of high design freedom and manufacturing flexibility. The PSI can then be customized to the unique anatomical geometry of individual patients, with various fixation with screws and plates for the initial stable fixation and porous lattice structures at the bone–implant junction to achieve osseointegration for the implant longevity. The design can also be biomechanically optimized by Finite Element Analysis (FEA) under patient-specific loading conditions before the actual manufacture [41,48,49]. The ideal PSI can only be realized under the close collaboration between the surgical teams and industrial sectors [50].

The cost-effectiveness of using the new technology is a concern, as the time for preoperative preparation, the CN setup, the design, and the fabrication of PSG require costly facilities and expertise with specialized skills that most tumor institutions do not have. Implants-related complications are expected to increase in time with surviving young bone sarcoma patients. However, joint-preserving implants have no mobile articulating joint components that wear in time as in traditional joint-sacrificing tumor implants. It remains determined if the accurate placement of joint-preserving implants with the retained natural joints can achieve better long-term limbs function and reduce future revision surgery. Therefore, the actual clinical efficacy needs further validation in a large number of patients with long-term outcomes or a prospective

design with a head-by-head comparison with approaches such as CN alone.

In selected patients with bone sarcomas, the described digital workflow and the NAVIG technique that combines both CN and PSG strengths may precisely replicate the complex surgical planning of geometric multiplanar bone tumor resections. It ensures the best fit between the PSG and the host bone without compromising local oncological clearance. The retained natural joint and the secondary osseointegration may allow better limb functions with more extended implant longevity. However, the current lack of a unified and simplified digital platform hinders popularity. A long-term follow up with more patients is also needed to determine the clinical efficacy of the digital approach and the new technique in joint-preserving tumor surgery.

## Funding

This research did not receive any specific grant from funding agencies in the public, commercial, or not-for-profit sectors.

## Declaration of competing interest

The author(s) have no conflicts of interest relevant to this article.

## Acknowledgement

We thank the senior implant design engineer, Mr. Michael Stockdale (Senior Staff Engineer, Product Development) and the Design Team, Stryker Elstree, Stanmore Implants, UK for the design and manufacture of the Patient-Specific Implants in this study. We also thank Mr. Brian HW Yeung, (Associate Sale Manager, Stryker China Limited) for his technical support of intraoperative use of the computer navigation system.

## References

- [1] Fuchs B, Hoekzema N, Larson DR, Inwards CY, Sim FH. Osteosarcoma of the pelvis: outcome analysis of surgical treatment. *Clin Orthop Relat Res* 2009;467:510–8.
- [2] Bertrand TE, Cruz A, Binitie O, Cheong D, Letson GD. Do surgical margins affect local recurrence and survival in extremity, nonmetastatic, high-grade osteosarcoma? *Clin Orthop Relat Res* 2016;474(3):677–83.
- [3] He F, Zhang W, Shen Y, Yu P, Bao Q, Wen J, et al. Effects of resection margins on local recurrence of osteosarcoma in extremity and pelvis: systematic review and meta-analysis. *Int J Surg* 2016;36(Pt A):283–92.
- [4] Agarwal M, Puri A, Anchan C, Shah M, Jambhekar N. Hemicyclic excision for low-grade selected surface sarcomas of bone. *Clin Orthop Relat Res* 2007;459:161–6.
- [5] Avedian RS, Haydon RC, Peabody TD. Multiplanar osteotomy with limited wide margins: a tissue preserving surgical technique for high-grade bone sarcomas. *Clin Orthop Relat Res* 2010;468:2754–64.
- [6] Deijkers RL, Bloem RM, Hogendoorn PC, Verlaan JJ, Kroon HM, Taminiau AH. Hemicyclic allograft reconstruction after resection of low-grade malignant bone tumours. *J Bone Joint Surg Br* 2002;84:1009–14.
- [7] Cho HS, Oh JH, Han I, Kim HS. Joint-preserving limb salvage surgery under navigation guidance. *J Surg Oncol* 2009;100(3):227–32.
- [8] Li J, Wang Z, Guo Z, Chen GJ, Yang M, Pei GX. Irregular osteotomy in limb salvage for juxta-articular osteosarcoma under computer-assisted navigation. *J Surg Oncol* 2012;106(4):411–6.
- [9] Wong KC, Kumta SM. Joint-preserving tumor resection and reconstruction using image-guided computer navigation. *Clin Orthop Relat Res* 2013;471(3):762–73.
- [10] Li J, Wang Z, Guo Z, Chen GJ, Yang M, Pei GX. Precise resection and biological reconstruction under navigation guidance for young patients with juxta-articular bone sarcoma in lower extremity: preliminary report. *J Pediatr Orthop* 2014 Jan; 34(1):101–8.
- [11] Aponte-Tinco LA, Ritacco LE, Ayerza MA, Muscolo DL, Farfalli GL. Multiplanar osteotomies guided by navigation in chondrosarcoma of the knee. *Orthopedics* 2013;36(3):e325–30.
- [12] Wong KC, Kumta SM. Computer-assisted tumor surgery in malignant bone tumors. *Clin Orthop Relat Res* 2013;471(3):750–61.
- [13] Jeys L, Matharu GS, Nandra RS, Grimer RJ. Can computer navigation-assisted surgery reduce the risk of an intralesional margin and reduce the rate of local recurrence in patients with a tumour of the pelvis or sacrum? *Bone Joint Lett J* 2013;95-B(10):1417–24.
- [14] Wong KC, Kumta SM, Sze KY, Wong CM. Use of a patient specific CAD/CAM surgical jig in extremity bone tumor resection and custom prosthetic reconstruction. *Comput Aided Surg* 2012;17(6):284–93.
- [15] Gouin F, Paul L, Odri GA, Cartiaux O. Computer-assisted planning and patient-specific instruments for bone tumor resection within the pelvis: a series of 11 patients. *Sarcoma* 2014:842709.

- [16] Jentzsch T, Vlachopoulos L, Fürnstahl P, Müller DA, Fuchs B. Tumor resection at the pelvis using three-dimensional planning and patient-specific instruments: a case series. *World J Surg Oncol* 2016 Sep 21;14(1):249.
- [17] Evrard R, Schubert T, Paul L, Docquier PL. Resection margins obtained with patient-specific instruments for resecting primary pelvic bone sarcomas: a case-control study. *Orthop Traumatol Surg Res* 2019 Jun;105(4):781–7.
- [18] Jud L, Müller DA, Fürnstahl P, Fucntese SF, Vlachopoulos L. Joint-preserving tumour resection around the knee with allograft reconstruction using three-dimensional preoperative planning and patient-specific instruments. *Knee* 2019 Jun;26(3):787–93.
- [19] Wong KC, Sze KY, Wong IO, Wong CM, Kumta SM. Patient-specific instrument can achieve same accuracy with less resection time than navigation assistance in periacetabular pelvic tumor surgery: a cadaveric study. *Int J Comput Assist Radiol Surg* 2016 Feb;11(2):307–16.
- [20] Bosma SE, Wong KC, Paul L, Gerbers JG, Jutte PC. A cadaveric comparative study on the surgical accuracy of freehand, computer navigation, and patient-specific instruments in joint-preserving bone tumor resections. *Sarcoma* 2018;4065846. 2018 Nov 13.
- [21] Wong KC, Kumta SM, Leung KS, Ng KW, Ng EW, Lee KS. Integration of CAD/CAM planning into computer assisted orthopaedic surgery. *Comput Aided Surg* 2010;15: 65–74.
- [22] Wong KC, Kumta SM, Antonio GE, Tse LF. Image fusion for computer-assisted bone tumor surgery. *Clin Orthop Relat Res* 2008 Oct;466(10):2533–41.
- [23] Enneking WF, Dunham W, Gebhardt MC, Malawar M, Pritchard DJ. A system for the functional evaluation of reconstructive procedures after surgical treatment of tumors of the musculoskeletal system. *Clin Orthop Relat Res* 1993;286:241–6.
- [24] Jeys LM, Kulkarni A, Grimer RJ, Carter SR, Tillman RM, Abudu A. Endoprosthetic reconstruction for the treatment of musculoskeletal tumors of the appendicular skeleton and pelvis. 1265–127 *J Bone Joint Surg Am* 2008;90.
- [25] Fu H, Yan CH, Cheung A, Cheung MH, Chan VWK, Chan PK, et al. Robotic-arm assistance simplifies hip arthrodesis conversion to total hip arthroplasty. *Arthroplasty Today* 2020;6:877–87.
- [26] Zhang Y, Zhang Q, Zhong LS, Qiu L, Xu LH, Sun Y, et al. New perspectives on surgical accuracy analysis of image-guided bone tumour resection surgery. *Int Orthop* 2020;44:987–94.
- [27] Kumta SM, Chow TC, Griffith J, Li CK, Kew J, Leung PC. Classifying the location of osteosarcoma with reference to the epiphyseal plate helps determine the optimal skeletal resection in limb salvage procedures. *Arch Orthop Trauma Surg* 1999;119: 327–31.
- [28] Hamed Kassem Abdelaal A, Yamamoto N, Hayashi K, Takeuchi A, Miwa S, Tsuchiya H. Epiphyseal sparing and reconstruction by frozen bone autograft after malignant bone tumor resection in children. *Sarcoma* 2015;2015:892141.
- [29] Aponte-Tinao L, Ayerza MA, Muscolo DL, Farfalli GL. Survival, recurrence, and function after epiphyseal preservation and allograft reconstruction in osteosarcoma of the knee. *Clin Orthop Relat Res* 2015;473:1789–96.
- [30] Li J, Wang Z, Ji C, Chen G, Liu D, Zhu H. What are the oncologic and functional outcomes after joint salvage resections for juxtaarticular osteosarcoma about the knee? *Clin Orthop Relat Res* 2017 Aug;475(8):2095–104.
- [31] Mankin HJ, Hornicek FJ, Rosenberg AE, Harmon DC, Gebhardt MC. Survival data for 648 patients with osteosarcoma treated at one institution. *Clin Orthop Relat Res* 2004;429:286–91.
- [32] Bacci G, Longhi A, Versari M, Mercuri M, Riccoli A, Picci P. Prognostic factors for osteosarcoma of the extremity treated with neoadjuvant chemotherapy: 15-year experience in 789 patients treated at a single institution. *Cancer* 2006;106(5): 1154–61.
- [33] Pakos EE, Nearchou AD, Grimer RJ, Koumoullis HD, Abudu A, Bramer JA, et al. Prognostic factors and outcomes for osteosarcoma: an international collaboration. *Eur J Canc* 2009;45(13):2367–75.
- [34] Andreou D, Bielack SS, Carrle D, Kevric M, Kotz R, Winkelmann W, et al. The influence of tumor- and treatment-related factors on the development of local recurrence in osteosarcoma after adequate surgery. An analysis of 1355 patients treated on neoadjuvant Cooperative Osteosarcoma Study Group protocols. *Ann Oncol* 2011;22:1228–35.
- [35] Andreou D, Bielack SS, Carrle D, Kevric M, Kotz R, Winkelmann W, et al. Survival from high-grade localised extremity osteosarcoma: combined results and prognostic factors from three European Osteosarcoma Intergroup randomised controlled trials. *2012 Ann Oncol* 2012;23(6):1607–16.
- [36] Fujiwara T, Sree DV, Stevenson J, Kaneuchi Y, Parry M, Tsuda Y, et al. Acetabular reconstruction with an ice-cream cone prosthesis following resection of pelvic tumors: does computer navigation improve surgical outcome? *J Surg Oncol* 2020; 121:1104–14.
- [37] Fujiwara T, Kaneuchi Y, Stevenson J, Parry M, Kurisunkal V, Clark R, et al. Navigation-assisted pelvic resections and reconstructions for periacetabular chondrosarcomas. *Eur J Surg Oncol* 2021 Feb;47(2):416–23.
- [38] Gupta A, Pollock R, Cannon SR, Briggs TWR, Skinner J, Blunn GW. A knee-sparing distal femoral endoprosthesis using hydroxyapatite-coated extracortical plates: preliminary results. *J Bone Joint Surg* 2006;88-B(10):1367–72.
- [39] Spiegelberg BGI, Sewell MD, Aston WJS, Blunn GW, Pollock R, Cannon SR, et al. The early results of joint-sparing proximal tibial replacement for primary bone tumours, using extracortical plate fixation. *J Bone Joint Surg* 2009;91-B(10): 1373–7.
- [40] Agarwal M, Puri A, Gulia A, Reddy K. Joint-sparing or physal-sparing diaphyseal resections: the challenge of holding small fragments. *CORR* 2010;468(11):2924–32.
- [41] Wong KC, Kumta SM, Geel NV, Demol J. One-step reconstruction with a 3D-printed, biomechanically evaluated custom implant after complex pelvic tumor resection. *Comput Aided Surg* 2015;20(1):14–23.
- [42] Wang B, Hao Y, Pu F, Jiang W, Shao Z. Computer-aided designed, three dimensional-printed hemipelvic prosthesis for peri-acetabular malignant bone tumour. *Int Orthop* 2018;42(3):687–94.
- [43] Angelini A, Trovarelli G, Berizzi A, Pala E, Breda A, Ruggieri P. Three-dimension-printed custom-made prosthetic reconstructions: from revision surgery to oncologic reconstructions. *Int Orthop* 2019 Jan;43(1):123–32.
- [44] Park JW, Kang HG, Kim JH, Kim HS. New 3-dimensional implant application as an alternative to allograft in limb salvage surgery: a technical note on 10 cases. *Acta Orthop* 2020;91(4):489–96.
- [45] Zhu D, Fu J, Wang L, Guo Z, Wang Z, Fan H. Reconstruction with customized, 3D-printed prosthesis after resection of periacetabular Ewing's sarcoma in children using "triradiate cartilage-based" surgical strategy: a technical note. *J Orthopaedic Trans* 2021;28:108–17.
- [46] Wyatt MC. Custom 3D-printed acetabular implants in hip surgery—innovative breakthrough or expensive bespoke upgrade? *Hip Int* 2015;25(4):375–9.
- [47] Hao Y, Wang L, Jiang W, Wu W, Ai S, Shen L, et al. 3D printing hip prostheses offer accurate reconstruction, stable fixation, and functional recovery for revision total hip arthroplasty with complex acetabular bone defect. *Engineering* 2020 Nov;6(11): 1285–90.
- [48] Du R, Su YX, Yan Y, Choi WS, Yang WF, Zhang C, et al. A systematic approach for making 3D-printed patient-specific implants for craniomaxillofacial reconstruction. *Engineering* 2020;6(11):1291–301.
- [49] Wang Y, Tan Q, Pu F, Boone D, Zhang M. A review of the application of additive manufacturing in prosthetic and orthotic clinics from a biomechanical perspective. *Engineering* 2020;6(11):1258–66.
- [50] Qiu G, Ding W, Tian W, Qin L, Zhao Y, Zhang L, et al. Medical additive manufacturing: from a frontier technology to the research and development of products. *Engineering* 2020;6(11):1217–21.